HHS Public Access

Author manuscript

Glia. Author manuscript; available in PMC 2017 January 01.

Published in final edited form as:

Glia. 2016 July ; 64(7): 1138–1153. doi:10.1002/glia.22987.

Radial Glia Inhibit Peripheral Glial Infiltration into the Spinal Cord at Motor Exit Point Transition Zones

Cody J. Smith[1], **Kimberly Johnson**[3], **Taylor G. Welsh**[1,2], **Michael J. F. Barresi**[3,4], and **Sarah Kucenas**[1,2]

[1]Department of Biology, University of Virginia, Charlottesville, Virginia 22904

[2]Neuroscience Graduate Program, University of Virginia, Charlottesville, Virginia 22904

[3]Department of Biological Sciences, Smith College, Northampton, Massachusetts 01003

[4]Molecular and Cellular Biology Graduate Program, University of Massachusetts, Amherst, Massachusetts 01003

Abstract

In the mature vertebrate nervous system, central and peripheral nervous system (CNS and PNS, respectively) GLIA myelinate distinct motor axon domains at the motor exit point transition zone (MEP TZ). How these cells preferentially associate with and myelinate discrete, non-overlapping CNS versus PNS axonal segments, is unknown. Using in vivo imaging and genetic cell ablation in zebrafish, we demonstrate that radial glia restrict migration of PNS glia into the spinal cord during development. Prior to development of radial glial endfeet, peripheral cells freely migrate back and forth across the MEP TZ. However, upon maturation, peripherally located cells never enter the CNS. When we ablate radial glia, peripheral glia ectopically migrate into the spinal cord during developmental stages when they would normally be restricted. These findings demonstrate that radial glia contribute to both CNS and PNS development and control the unidirectional movement of glial cell types across the MEP TZ early in development.

Keywords

motor exit point glia; CNS/PNS transition zone; radial glia; zebrafish; neural crest cells

Introduction

The nervous system is segregated into the CNS and PNS. Within each half of the nervous system, there are unique glial populations that have redundant functions. In the CNS, oligodendrocytes myelinate axons while in the PNS, Schwann cells, and MEP glia perform this function (Emery, 2010; Fraher and Rossiter, 1983; Jessen and Mirsky, 2005; Smith et al., 2014). Intriguingly, in several disease states, this clear cellular segregation of the nervous system is disrupted (Itoyama et al., 1983; Maro et al., 2004; Coulpier et al., 2009). How

Address correspondence to Sarah Kucenas, Department of Biology, Physical and Life Sciences Building, Rm 312, PO Box 400328, University of Virginia, Charlottesville, VA 22904-4328. sk4ub@virginia.edu.

Additional Supporting Information may be found in the online version of this article.

these boundaries are established and more specifically, how migratory peripheral glia are restricted from entering the spinal cord during normal development, is not understood.

Recently, we and others identified cells that function at spinal cord boundaries to keep CNS and PNS cell populations segregated (Coulpier et al., 2010; Smith et al., 2014). In mammals, neural crest-derived boundary cap cells prevent spinal cord neurons from exiting the CNS and are hypothesized to also play a role in glial segregation (Coulpier et al., 2010; Vermeren et al., 2003). We recently identified a CNS-derived peripheral glial population, MEP glia, which function to restrict oligodendrocyte progenitor cell (OPC) migration out of the spinal cord (Smith et al., 2014). Although there are several studies investigating the migration of cells out of the CNS, ectopic migration of peripheral cells into the spinal cord is much less understood. Typically, ectopic entry of peripheral cells into the spinal cord is correlated with the disruption of astrocytes in mature nervous systems (Blakemore and Patterson, 1975; Blakemore, 1976; Duncan et al., 1988; Duncan and Hoffman, 1997). Whether cells are restricted at this boundary during development, prior to astrocyte specification, is not known.

To determine what restricts the migration of cells into the spinal cord during development, we used live imaging in zebrafish, coupled with cell-specific genetic ablation. We show that radial glia function to establish and maintain glial segregation at the spinal MEP TZ. We demonstrate that prior to radial glial maturation, PNS cells at the MEP freely migrate into and back out of the spinal cord. However, once radial glia elaborate endfeet along the basal edge of the spinal cord, this migration ceases. When we ablate radial glia during early nervous system development, PNS glia at the MEP ectopically migrate back into the spinal cord. We conclude that during development, radial glia are essential to control unidirectional and selective glial migration across the MEP TZ.

Materials and Methods

Fish Husbandry

All animal studies were approved by the University of Virginia Institutional Animal Care and Use Committee. Zebrafish strains used in this study were: AB*, *Tg(gfap:nsfB-mcherry)* (Johnson et. al, companion paper), *Tg(sox10(4.9):eos)* (Prendergast et al., 2012), *Tg(sox10(4.9):nls-eos)* (McGraw et al., 2012), *Tg(olig2:dsred)*^{vu19} (Park et al., 2002), *Tg(pU1:gal4, UAS:egfp)* (Peri and Nüsslein-Volhard, 2008), *Tg(gfap:egfp)*^{mi2001} (Bernardos and Raymond, 2006b) and *Tg(mpeg1:egfp)* (Ellett et al., 2011). Abbreviations used for each line are listed in Table 1. Pairwise matings were used to produce embryos that were raised at 28.5°C in egg water and staged by hours or days post fertilization (hpf and dpf, respectively). Embryos of either sex were used for all experiments (Kimmel et al., 1995). Phenylthiourea (PTU) (0.004%) in egg water was used in immunohistochemistry and live imaging to reduce pigmentation. Stable, germline transgenic lines were used in all experiments.

In Vivo Imaging

Embryos were manually dechorionated at 24 hpf and treated with PTU as described above. For imaging, embryos were anesthetized with 3-aminobenzoic acid ester (Tricaine), immersed in 0.8% low-melting point agarose and mounted laterally in glass-bottomed 35 mm petri dishes (Electron Microscopy Sciences). A 25X multi-immersion objective (NA = 0.8), 40X oil objective (NA= 1.4), 40X water objective (NA = 1.1) or a 63X water objective (NA = 1.2) mounted on a motorized Zeiss AxioObserver ZI microscope equipped with a Quorum WaveFX-XI spinning disc confocal system (Quorum Technologies Inc.) was used to capture images. Image processing was done with Metamorph and Photoshop, which were used to enhance brightness and contrast of images. Supporting Information videos were annotated using ImageJ trackM plugin.

Sectioning Embryos

Animals at the appropriate age were fixed in 4% PFA for 3 h at room temperature (25°C), mounted in sectioning agar and then placed in 30% sucrose overnight at 4°C or until the block was saturated. Blocks were then frozen and sectioned via cryosectioning. 20 μm sections were taken of the trunk and placed onto a slide for immunohistochemistry.

Immunohistochemistry

Animals were with fixed and stained as previously described (Smith et al., 2014). The primary antibodies used in this study include: Sox10–1:5,000 (Binari et al., 2013), Isl1-1:100 (Developmental Studies Hybridoma Bank at the University of Iowa), Acetylated Tubulin 1:10,000 (Sigma), Caspase-1:600 (BD Biosciences) and Zrf-1–1:250 (Developmental Studies Hybridoma Bank at the University of Iowa). The secondary antibodies include Alexa antibodies 1:600 (Invitrogen): goat anti-rabbit 568, goat anti-mouse 568, goat anti-rabbit 647 and goat anti-mouse 647. After staining, animals were stored in 50% glycerol/50% 1X PBS at 4°C until mounted under a bridged coverslip and imaged.

Eos Photoconversion

Animals were treated with PTU as described above and mounted for *in vivo* imaging. As previously described to distinguish neural crest versus MEP glia (Smith et al., 2014), *Tg(sox10:eos)* embryos were exposed to UV light using a DAPI filter for 20 – 30 s with an Zeiss axiozoom microscope at 48 hpf. To convert only PNS located cells, animals were mounted for *in vivo* imaging. Animals were positioned on the confocal microscope such that the spinal cord was out of the field of view and therefore, only PNS cells were exposed to UV light. Photoconversion was done with a 491 laser and DAPI filter set. Successful photoconversion of PNS cells was confirmed immediately following photconversion by imaging the entire trunk region with red and green filter sets.

Radial Glia Ablation

Tg(gfap:nsfB-mcherry) embryos were exposed to 10 mM Metronidazole (MTZ) solution (10 mM Metronidazole, 0.2-2% DMSO) in egg water (before 24 hpf) or PTU (after 24 hpf) (Curado et al., 2008). Reduction of mCherry fluorescence was confirmed using the RFP

filter set on a Zeiss AxioZoom microscope. Fresh Metronidazole solution was replaced every 24 h. Control embryos were exposed to 0.2-2% DMSO.

Confirmation of CNS-Located PNS Glia

Tg(sox10:nls-eos) embryos were treated with 10 mM Metronidazole solution at 24 hpf and mounted at 56 hpf as described above. Using confocal microscopy, PNS-located cells were exposed to UV light as discussed above, unmounted and grown until 80 hpf at 28.5°C, fixed in 4% PFA for 3 h at room temperature (25°C) and then 25-μm sections were collected of the trunk, as described above. These sections were then imaged using a 40X oil objective on a Zeiss AxioObserver ZI microscope equipped with a Quorum WaveFX-XI spinning disc confocal system (Quorum Technologies Inc.) with both 491 and 561 laser lines and GFP and RFP filter sets. Merged images were processed using Metamorph to distinguish photoconverted versus unconverted cells.

Scoring OPC Location

Tg(olig2dsred) embryos were fixed and stained at different developmental times with antibodies specific to Sox10 and acetylated tubulin to distinguish CNS cell-types as described above. *olig2*$^{+}$/Sox10^{+} cell position was scored in sections where the motor nerves could be visualized exiting the spinal cord. Cells were scored at the MEP if they were located where the motor axons, labeled with acetylated tubulin, exit the spinal cord.

OPC Ablation

Tg(sox10:eos) embryos were exposed to 100 ng/ml of Trichostain A (TSA) in egg water or PTU at 24 or 36 hpf (Takada and Appel, 2010). Time-lapse imaging of these embryos was performed at 48 hpf. A reduction of OPCs was confirmed by loss of Eos^{+} cells within the spinal cord. Control embryos were exposed to 0.2 – 2% DMSO.

Quantification of Immune Cells

Tg(pU1:egfp);Tg(gfap:nsfB-mcherry) or *Tg(mpeg1:egfp);Tg(gfap:nsfB-mcherry)* embryos were treated with DMSO or MTZ at 24 hpf and then imaged at 72 hpf or 5 dpf. Confocal images were captured using a 40X water objective. In these studies, 6 animals per genotype were used and 6 images of the spinal cord were taken. Scoring was completed by dividing the spinal cord into equal thirds (ventral, middle, dorsal) and the presence or absence of cells was scored per spinal cord image. Transverse sections were used to confirm location of immune cells within the spinal cord.

Data Quantification and Statistical Analysis

All cell counts and analyses were done with composite Z image stacks compiled using Metamorph software. Individual z images were sequentially observed and cells counted within the entire z stack. All graphically presented data represent the mean of the analyzed data. GraphPad Prism software was used to determine statistical analysis. A Chi-squared two-tailed test using a confidence interval of 95% was used to determine the level of significance.

Results

Myelinating Glia Are Segregated at the MEP TZ

In the mature nervous system, myelinating glia in the CNS and PNS are segregated at the MEP TZ (Fraher and Kaar, 1986; Fraher, 1997). To investigate what prevents migration of cells into the spinal cord, we imaged the MEP TZ during spinal motor nerve assembly. For the purpose of this paper, we define MEP TZs as the points in the nervous system where motor axons cross between the spinal cord and periphery and both central and peripheral cell types converge. Spinal MEP TZs are positioned in the middle of each somite hemisegment in a repeated pattern along the anterior-posterior axis of the developing zebrafish embryo (Fig. 1A,B). Using stable transgenic lines that use *sox10* and *olig2* regulatory sequences to drive expression of Eos and DsRed, respectively, we were able to label all of the distinct neuronal and glial populations located near the MEP at the earliest stages of motor nerve assembly (Park et al., 2002; Prendergast et al., 2012). In *Tg(olig2:dsred);Tg(sox10:eos)* embryos, neural crest-derived glia and their precursors were $sox10^{+}$ (green), OPCs expressed *olig2* and *sox10* and motor neurons and their axons were $olig2^{+}$. Therefore, in this transgenic combination, the three major cell types at the nascent MEP were differentially labeled, with neural crest in green, OPCs in yellow and motor neurons and their axons in red (Fig. 1B). To visualize cell dynamics at the MEP, we first imaged embryos at 24, 48 and 72 hours post fertilization (hpf), the developmental stages when PNS cells migrate to the MEP, proliferate and differentiate into mature cell types (Raible et al., 1992; Smith et al., 2014). At 24 hpf, as previously described, we observed $sox10^{+}$ neural crest cells closely associated with outgrowing $olig2^{+}$ motor axons, but OPCs were not yet specified at this stage (Fig. 1B,C). By 48 hpf, spinal cord gliogenesis had begun and we observed $olig2^{+}/sox10^{+}$ OPCs in the CNS while $sox10^{+}$ neural crest-derived cells remained on the peripheral side of the MEP (Fig. 1B,D). Ultimately, by 72 hpf, $sox10^{+}/olig2^{+}$ OPCs were located throughout the spinal cord, with a subset associated with motor axons on the central side of the MEP TZ, closely juxtaposed to $sox10^{+}$ MEP glia in the periphery along the same axon (Fig. 1B,E). $sox10^{+}$ neural crest-derived Schwann cells were also associated with distal spinal motor axon segments (data not shown). Previously, we showed that MEP glia are a CNS-derived peripheral glial population that migrates out of the spinal cord via the MEP TZ at approximately 52 hpf and proliferates, giving rise to myelinating glia that ensheath spinal motor root axons, replacing neural crest cells as the PNS cell that resides closest to the MEP (Smith et al., 2014). After this stage, OPCs, MEP glia and neural crest-derived Schwann cell precursors go on to differentiate into their respective mature myelinating populations and remain strictly segregated to either the CNS or PNS (Raible and Eisen, 1994; Park et al., 2002; Smith et al., 2014) (data not shown). To determine if glial mixing across the MEP TZ occurred during these discrete stages of development, we digitally rotated our confocal z-stacks 90 degrees to visualize a cross-section of the spinal cord (Fig. 1B). This new view of the developing MEP TZ showed that at these stages, OPCs and peripherally-located glia were segregated at the MEP and never appeared to co-mingle (Fig. 1C–E).

PNS Cells Migrate into the Spinal Cord during Early Development

Based on our analysis between 24 and 72 hpf, we hypothesized that CNS and PNS glial precursors either: (1) directly migrate to their final locations or (2) are influenced by

mechanisms that ensure they end up on the correct side of the MEP during development. Previously, we and others demonstrated that OPCs survey their immediate environment, both centrally and peripherally, by extending and retracting filipodial-like processes before ultimately myelinating CNS axon segments (Kirby et al., 2006; Hughes et al., 2013; Smith et al., 2014). This surveying activity is thought to not only properly space OPCs within the spinal cord, but also serves to keep them within the CNS (Smith et al., 2014).

To determine if peripheral glial precursors sample their environment in a similar way to developing OPCs, we used time-lapse imaging to continuously observe the developing MEP TZ in *Tg(sox10:nls-eos);Tg(olig2:dsred)* embryos between 24 and 72 hpf. We hypothesized that if a surveying mechanism contributed to glial segregation on the peripheral side of the MEP (Smith et al., 2014), then we might visualize peripheral glial precursors exploring the CNS. In our imaging at 24 hpf, we observed *sox10*$^{+}$ PNS cells exploring the peripheral segment of motor axons, as previously described (Honjo et al., 2008; McGraw et al., 2012; Smith et al., 2014) (data not shown). However, unlike in the static images presented above, *in vivo*, time-lapse imaging between 24 and 48 hpf revealed that *sox10*$^{+}$ PNS cells migrate into the CNS (33% of nerves imaged, n = 9) by pinching through the MEP TZ (Fig. 2A,C, Movie 1). In 100% of these instances, the CNS-located peripheral cell-type always migrated back into the periphery by pinching back through the MEP TZ within 2 hours (Fig. 2, Movie 1). This pinching behavior is reminiscent of cells migrating across the MEP TZ and represents a migratory event between the CNS and PNS (Kucenas et al., 2008; Kucenas et al., 2009; Smith et al., 2014). When we digitally rotated these z-projections 90 degrees to visualize a cross section of the embryo, we confirmed that these *sox10*$^{+}$ nuclei were briefly within the spinal cord before migrating back into the periphery, where they remained for the rest of the imaging period (Fig. 2B). From these results, we conclude that at least a subpopulation of PNS cells can survey both the CNS and PNS during development.

One hypothesis to explain this ectopic migration we observed between 24 and 48 hpf is that there is not a “do not enter” mechanism present during this developmental stage. To directly test if such a mechanism eventually exists, we investigated if the ectopic migration of PNS cells persisted throughout development, or if there was a temporal window when cellular restriction was established. To investigate this, we imaged PNS cells in *Tg(sox10:nls-eos);Tg(olig2:dsred)* embryos after 48 hpf at the MEP and scored the number of migratory *sox10*$^{+}$ PNS cells that entered spinal cord. Unlike earlier stages of development, we never (n > 20 nerves) visualized PNS cells enter the spinal cord between 48 and 72 hpf (Fig. 2C). These results are consistent with the hypothesis that the MEP TZ is permeable to cells entering the spinal cord prior to 48 hpf and that cellular restriction at the MEP is established by 48 hpf.

OPCs Are Unlikely to Restrict Peripheral Cell Migration into the Spinal Cord

At 48 hpf, we observed a dramatic change in the exploratory behavior of PNS cells into the spinal cord. Therefore, we hypothesized that their lack of central migration after this stage was mediated by the presence of a spinal cord cell population that repelled them. Previously, we and others have shown that contact-mediated inhibition between OPCs and PNS glia restrict OPCs to the spinal cord during development (Coulpier et al., 2010; Smith et al.,

2014). Therefore, we hypothesized that the cells responsible for restricting peripheral glial precursor migration into the spinal cord were OPCs. To test this hypothesis, we imaged the development of OPCs between 24 and 72 hpf. Using *Tg(olig2:dsred)* embryos, we stained transverse sections of the trunk spinal cord with an antibody specific to Sox10, a marker of OPCs, MEP glia and neural crest-derived Schwann cells (Binari et al., 2013). At 24 hpf, consistent with previously published studies, we did not visualize any $Sox10^{+}/olig2^{+}$ cells in the spinal cord, as OPCs aren't specified until later in development (Park et al., 2002) (Fig. 3A). By 48 hpf, we observed a small number of $Sox10^{+}/olig2^{+}$ OPCs within the spinal cord (Fig. 3A). To more closely investigate their location relative to the MEP TZ, we scored their position (dorsal versus ventral and medial versus lateral) and observed >1 OPC per section near the MEP at 48 hpf (Fig. 3A,B). These results are consistent with the hypothesis that OPCs at 48 hpf are not in a location that allows them to directly repel ectopically migrating PNS cells. By 72 hpf, the OPC population was much larger and these cells were dispersed evenly throughout the spinal cord, including ventral positions immediately adjacent to MEP TZs. Taken together, these data are consistent with the hypothesis that OPCs are unlikely to be the CNS cell population that restricts PNS cell migration. However, we acknowledge that despite the fact that we never observed $Sox10^{+}$ cell bodies at the MEP, OPC processes from OPCs in the ventral spinal cord could potentially extend towards the MEP TZ and restrict PNS cells from migrating into the spinal cord. To our knowledge, there is not a unique marker for OPC processes that allows us to investigate this possibility at this time.

Therefore, we used an additional experimental paradigm to test the hypothesis that OPCs are dispensable for PNS cell restriction at the MEP TZ. To do this, we first treated *Tg(sox10:eos)* embryos from 36 to 72 hpf with a histone deacetylase (HDAC) inhibitor, Trichostatin A (TSA), which blocks OPC specification (Takada and Appel, 2010). In TSA-treated larvae, we did not visualize any $sox10^{+}$ OPCs in the spinal cord, confirming the efficacy of the drug treatment (Fig. 3C). To determine if the lack of OPCs altered the ability of PNS cells to ectopically migrate into the spinal cord, we used time-lapse imaging. In movies taken from *Tg(sox10:eos)* TSA-treated embryos between 48 and 72 hpf, we never observed peripheral cells migrate into the spinal cord, even though PNS cells were present in the periphery along spinal motor root axons (Fig. 3C, Movie 2) ($n = 6$ movies). As a control to ensure that our TSA treatment was not also inhibiting the migration of PNS cells, we treated *Tg(sox10:eos)* embryos at 24 hpf and imaged from 24 to 48 hpf, when we previously observed neural crest cells ectopically migrating into the spinal cord. In these movies, TSA-treated embryos had normal neural crest migration from the dorsal spinal cord to the MEP TZ, and $sox10^{+}$ PNS cells migrated into and back out of the spinal cord in a manner indistinguishable from the data we presented above (data not shown) (22% of nerves imaged, $n = 18$). Therefore, taken together, we conclude that OPCs are not the cell population that prevents the migration of peripheral glial precursors into the spinal cord.

Radial Glia Restrict Ectopic Peripheral Glial Migration into the CNS

We next hypothesized that the cell population that restricted peripheral glial migration into the CNS may also be glial in nature. In addition to OPCs, the other major glial population in the developing zebrafish spinal cord is radial glia (Bernardos and Raymond, 2006; Johnson et al., 2013; Kim et al., 2008). We reasoned that because radial glia line the basal edge of the

spinal cord with glial endfeet, they may function to restrict PNS cells from ectopically entering the spinal cord during development. To begin to address the role of radial glial cells in MEP TZ formation, we first characterized radial glial development at the MEP. To do this, we used *Tg(gfap:egfp)* embryos, which have EGFP under the control of *glial fibrillary acidic protein (gfap)* regulatory sequences (Bernardos and Raymond, 2006). At 24 hpf, radial glial morphology was columnar in nature and we did not observe mature glial endfeet or a clear demarcation of the basal edge of the spinal cord by these cells (Fig. 4A,B). At 36 hpf, this columnar morphology began to transition into a more polarized morphology and by 48 hpf, radial glial cells displayed a mature morphology with cell bodies positioned near the central canal and mature endfeet that extended to and lined the basal edge spinal cord (Fig. 4A,B). In higher magnification images of *Tg(gfap:egfp);Tg(olig2:dresd)* embryos at 24 and 48 hpf, radial glial endfeet were drastically more mature and noticeably demarcated the edge of the spinal cord at the MEP TZ at approximately 48 hpf, but not before (Fig. 4B). We confirmed these results using an antibody specific to radial glia, GFAP/Zrf-1 (data not shown) (Johnson et al., 2013). The maturation of radial glia and their endfeet at the MEP TZ correlate with the timing of peripheral cellular restriction from the spinal cord and led us to hypothesize that radial glial cells function to inhibit ectopic migration of peripheral glial cells into the CNS.

To test this hypothesis, we created a transgenic animal that allows for the specific ablation of radial glia (additional studies reported in Johnson et al., companion paper). This line uses a 7.4 kb piece of *gfap* regulatory sequence to drive expression of the nitroreductase B gene (*nfsB/NTR*), which encodes a bacterial enzyme that converts the normally nontoxic drug, Metrodinazole (MTZ), into a cytotoxic metabolite in radial glial cells (Fig. 4C). NTR is harmless when expressed in zebrafish, but when NTR^+ cells are exposed to MTZ, this enzyme triggers cell autonomous apoptosis and allows for both temporal and spatial control of cell ablation (Myers et al., 1986; Curado et al., 2008). We fused the coding sequence for mCherry to *nfsB* to visualize $gfap^+$ cells and monitor the timing and extent of radial glial death after addition of MTZ to the water (additional studies reported in Johnson et al., companion paper). In these embryos, we first confirmed that mCherry is expressed in $gfap^+$ radial glial cells by scoring the co-expression of an antibody specific to GFAP with NTR-mCherry (Fig. 4D). We then treated *Tg(gfap:nfsB-mcherry)* embryos with MTZ at 24 hpf and monitored cell death using the apoptotic marker anti-activated Caspase-3 (Fig. 4D). We chose treatment at 24 h because we hypothesized it would eliminate radial glia at approximately 48 hpf without disrupting the neural populations that are produced earlier in development by $gfap^+$ cells (as shown in our companion paper, Johnson et al.,) (Kim et al., 2008). To verify this, we labeled DMSO and MTZ-treated embryos 12 hours after treatment, at 36 hpf, with an anti-caspase-3 antibody and did not visualize widespread caspase staining (Fig. 4D). However, at 48 hpf, after 24 hours of MTZ treatment, radial glial cells throughout the spinal cord underwent apoptotic cell death (Fig. 4D). Compared to embryos treated with DMSO only, MTZ-treated embryos had significantly more Caspase-3^+ cells in the spinal cord (Fig. 4D). By 72 hpf, after 48 hours of MTZ-treatment, radial glial NTR-mcherry expression was nearly eliminated (Fig. 4D). Labeling with the ZRF-1 antibody, which labels all radial glia in the spinal cord, confirmed that radial glia expressing NTR underwent apoptosis, but radial glia in the floor plate, which are not labeled with this gfap promoter, do

not express NTR and do not die, providing evidence for the specificity of radial glia cell death (Fig. 4D) (Kim et al., 2008). We also wanted to determine if other spinal cord cell populations that are either produced by radial glia or depend on their presence, are disrupted in our treatment paradigm. To do this, we quantified the number of motor neurons and OPCs at 56 hpf, when we saw the highest level of radial glial cell death. Consistent with the hypothesis that radial glial ablation late, at 48 hpf, was not perturbing motor neuron specification, we observed a similar number of Isl^+ motor neurons in MTZ-treated and control embryos (Fig. 4E,F). Using a Sox10 antibody, we did observe a mild reduction, but not complete elimination, of OPCs in the spinal cord in MTZ-treated versus control embryos (Fig. 4G). These results demonstrate that in *Tg(gfap:nfsB-mcherry)* embryos treated with MTZ at 24 hpf, radial glial cells are targeted for ablation between 48 and 72 hpf, with no significant impact on motor neuron or OPC populations.

Although OPC number was slightly reduced in our ablation paradigm, the OPC studies we present above led us to rule out their involvement in restricting peripheral cells from entering the spinal cord. Given that radial glial endfeet are present at the MEP TZ at 48 hpf, when peripheral cellular restriction is established, we hypothesized that they function in segregating glia at this location. To test this hypothesis, we treated *Tg(gfap:nsfB-mcherry);Tg(sox10:eos)* embryos with MTZ at 24 hpf and imaged peripheral glial dynamics after cell ablation. Consistent with our previous analysis, we did not observe any cells migrate into the spinal cord in DMSO-treated control *Tg(gfap:nfsB-mcherry);Tg(sox10:eos)* embryos between 48 and 72 hpf. In contrast, during this same time period, we observed $sox10^+$ peripheral glial cells ectopically migrate into the spinal cord of MTZ-treated embryos starting at 48 hpf (33%, n = 6 nerves) (Fig. 5A,E). These $sox10^+$ cells pinched through the MEP TZ and unlike the PNS cells that ectopically entered between 24 and 48 hpf, remained in the spinal cord during the entire imaging period (48 to 72 hpf) (Fig. 5A, data not shown). We confirmed that in our treatment paradigm, radial glial endfeet were disrupted in 100% (n = 60 nerves) of the nerves by 56 hpf, when we visualized this ectopic migration (Fig 4). To further confirm that this ectopic migration of PNS cells into the spinal cord between 48 and 72 hpf was a result of radial glial ablation, we also imaged 24 hour MTZ-treated animals between 24 and 48 hpf, when MTZ had not yet induced radial glial death. In these movies, we visualized neural crest cells ectopically enter the spinal cord, but not at a higher frequency than non-treated animals (data not shown). These results support the hypothesis that radial glia restrict peripheral glia at the MEP from migrating into the spinal cord.

To confirm that peripheral cells are entering the CNS and not migrating ectopically along the outer edge of the spinal cord, we treated *Tg(gfap:nsfB-mcherry);Tg(sox10:nls-eos)* embryos with MTZ at 24 hpf and then used Eos-mediated fate mapping to differentially label central versus peripheral-located glia. The Eos protein, when exposed to ultraviolet (UV) light, irreversibly shifts its emission from a green fluorescent state (516 nm) to a red fluorescent state (581 nm) (Smith et al., 2014). Thus, Eos can be used to track cells over time. After treating embryos with MTZ at 24 hpf to ablate radial glial cells, we exposed only peripheral motor root-associated $sox10^+$ cells to UV light at 56 hpf, thus photoconverting spinal motor root associated glial cells from green to red (Fig. 5C). We then let the embryos mature, fixed them at 80 hpf and sectioned them to determine if photoconverted (red) $sox10^+$ peripheral

glia entered the spinal cord after radial glial ablation (Fig. 5D). In sections of MTZ-treated larvae, we observed photoconverted (red) *sox10*$^{+}$ cells within the spinal cord, whereas in control DMSO-treated larvae, we did not (n = 6) (Fig. 5D). We could distinguish the photoconverted Eos fluorescent cells from *mcherry*$^{+}$ radial glial debris because they also expressed low levels of unconverted Eos protein, a consequence of newly produced Eos that occurred during the time window from when it was photoconverted (56 hpf) to when we fixed the larvae (80 hpf) (Fig. 5D). We also always observed photoconverted *sox10*$^{+}$ cells in the periphery in both treated and nontreated larvae, demonstrating that not all PNS glia ectopically migrate into the spinal cord (Fig. 5D). Based on these findings, we conclude that PNS glia migrate into the spinal cord in the absence of radial glia.

We next asked if radial glial cells provide this restrictive function only during the stages when PNS glia are highly migratory, or if they continue to provide this restriction as a maintenance function. To address this, we treated *Tg(gfap:nsfB-mcherry);Tg(sox10:eos)* larvae with MTZ at 48 hpf. Time-lapse imaging of these embryos from 72 to 96 hpf, 24 h after MTZ treatment, showed that unlike DMSO-treated animals, PNS glia migrated into the spinal cord when radial glia were ablated at 72 hpf (Fig. 5B,E) (33%, n = 6 nerves). Based on these results, we conclude that radial glia function to not only establish, but also to maintain glial restriction at the MEP TZ.

The ectopic migration of PNS glia into the spinal cord in our radial ablation paradigm could be from the loss of restrictive boundary from radial glia at the MEP TZ, or from a strong entry signal such as cell damage. To distinguish between these two possibilities, we used a defraction-limited MicroPoint laser equipped with a coumarin 440 dye to create focal lesions either specifically at the MEP TZ where radial glia are present, or just dorsal to the MEP, where cells inside the spinal cord are damaged but the radial glial endfeet at the TZ would be undisturbed. We did these focal lesions in *Tg(sox10:eos)* animals either in combination with *Tg(olig2:dsred)* or *Tg(nbt:dsred)* transgenes, to visualize the lesion of neuronal cell types at the MEP. When we specifically ablated MEP TZ, we observed PNS glial cells extend dynamic processes into the spinal cord (Fig. S1A). In contrast, when we ablated cells just dorsal to the MEP, inside the spinal cord, we did not observe peripheral glial processes inside the CNS (Supp. Info. Figure S1B). These results are consistent with the hypothesis that ectopic migration of PNS glia into the spinal cord is likely from the loss of radial glia endfeet and not from a damage signal that induces PNS cells to enter the spinal cord.

MEP Glia Migrate into the Spinal Cord in the Absence of Radial Glia

Spinal motor nerve roots are populated with both centrally and peripherally derived glial populations (MEP glia and Schwann cells, respectively), suggesting that either cell-population is competent to enter the spinal cord (Smith et al., 2014). To determine which peripheral glial lineage, MEP glia, Schwann cells or both, ectopically enter the spinal cord after radial glia ablation, we used *Tg(sox10:eos);Tg(gfap:nsfB-mcherry)* embryos to ablate radial glial cells and then labeled centrally versus peripherally-derived PNS glia as previously described with UV light photoconversion (Smith et al., 2014) (Fig. 6A). We treated embryos with MTZ at 24 hpf and then specifically photoconverted only *sox10*$^{+}$

neural crest-derived cells at 48 hpf, as MEP glia are not yet specified at this stage (Fig. 6A) (Smith et al 2014). When we imaged these embryos at 72 hpf, neural crest-derived glia appeared yellow and were associated with developing dorsal root ganglia (DRG) and were never found in the spinal cord (Fig. 6B). In contrast, we observed unconverted (green) *sox10*$^{+}$ cells that had a morphology typical of MEP glia, and distinct from all other CNS glial cell types, within the spinal cord and not along the spinal motor root axons (Fig. 6B). From these data, we hypothesized that the unconverted *sox10*$^{+}$ cells in the MTZ-treated embryos were ectopically-located MEP glia because they were not present during photoconversion at 48 hpf and had a morphology distinct from OPCs (Fig. 6B,C). To more directly test this hypothesis, we used time-lapse imaging in these embryos between 48 and 72 hpf and observed unconverted (green) *sox10*$^{+}$ MEP glia normally exit the spinal cord at approximately 56 hpf (Fig. 6, Movie 3). However, unlike in DMSO-treated control embryos, MEP glia in MTZ-treated embryos pinched back through the MEP TZ and migrated anteriorly or posteriorly within the floor plate (Fig. 6D). In contrast, peripherally-derived neural crest glia, labeled as photoconverted Eos (red), were seen in the spinal cord much less often (Fig. 6C). These data demonstrate that upon radial glial ablation, centrally-derived MEP glia exit the spinal cord normally but then ectopically migrate back into the CNS, where they remain through at least 5 days post fertilization (dpf) (data not shown).

Immune Cells Do Not Interact with Ectopic Peripheral Glia in the CNS

In spinal cord demyelinating disease states, peripheral cells in ectopic spinal cord locations have been associated with active immune cells. We therefore asked if ectopic migration of MEP glia into the spinal cord correlated with the presence of immune cells. In the CNS, the major population of immune cells is microglia (Peri and Nüsslein-Volhard, 2008). To determine if microglia were recruited to areas where ectopic MEP glia reside, we imaged *Tg(gfap:nsfB-mcherry);Tg(pU1:egfp)* larvae, which use *pU1* regulatory sequences to drive expression of EGFP in microglial cells (Peri and Nüsslein-Volhard, 2008). We treated these embryos with MTZ at 24 hpf to ablate radial glia and then imaged them at 72 hpf, when MEP glia have ectopically migrated into the spinal cord. In control larvae, we did not visualize any microglia in the spinal cord at 72 hpf (Fig. 7A). In MTZ-treated embryos, however, we observed several microglia with multiple dendritic-like processes (Fig. 7A), a characteristic of activated microglial cells, within the spinal cord (Peri and Nüsslein-Volhard, 2008). We visualized mCherry^{+} puncta localized within these EGFP^{+} microglia, demonstrating that microglia were actively clearing radial glial debris created by MTZ-induced ablation (Fig. 7A). We confirmed that these EGFP^{+} cells were likely to be microglia and not macrophages that had infiltrated the spinal cord because when we ablated radial glia in *Tg(gfap:nsfB-mcherry);Tg(mpeg:egfp)* embryos, where *mpeg* regulatory sequences label peripheral macrophages with EGFP, we never saw EGFP^{+} cells inside the spinal cord (Fig. 7A).

To determine if these activated microglia interacted with ectopically-located PNS glia, we scored the location of microglia inside the spinal cord at 72 hpf in MTZ-treated larvae. In larvae lacking radial glia, we never observed microglia within the ventral third of the spinal cord where ectopic MEP glia were located (Fig. 7D). When we extended these studies to 5 dpf, after radial glial debris was cleared, we observed microglia in the CNS in both control

and MTZ-treated larvae. However, we only observed microglia in the dorsal third of the spinal cord and they were never associated with ectopically-located MEP glia (Fig. 7B–D). Based on this evidence, we conclude that ectopically-located MEP glia do not elicit a microglial or macrophage response.

Selective Restriction of Cell Migration at the MEP

We next hypothesized that radial glia may selectively restrict migration across the CNS/PNS boundary. To investigate this further, we sought to determine if radial glia also functioned to restrict cells from ectopically exiting the spinal cord. To do this, we imaged Tg(gfap:nsfB-mcherry);Tg(sox10:eos);Tg(olig2:dsred) embryos, which label motor neurons and OPCs with *olig2* (Park et al., 2002). We treated these embryos with MTZ at 24 hpf and imaged them at 72 hpf, when OPCs were previously observed ectopically exiting the spinal cord in the absence of MEP glia (n = 20) (Smith et al., 2014). In these studies, we did not visualize any *olig2*$^{+}$ motor neurons or *olig2*$^{+}$/*sox10*$^{+}$ OPCs in the periphery in MTZ-treated embryos (Fig. 8). These results suggest that disruption of radial glia in our paradigm does not generally perturb the CNS/PNS boundary and is consistent with the hypothesis that radial glia selectively restrict PNS glia from entering the spinal cord. Therefore, we conclude that radial glia control unidirectional and selective movement across the MEP TZ by preventing PNS glia from entering the spinal cord (Fig. 9).

Discussion

The CNS and PNS are typically thought of as segregated halves that are functionally and anatomically linked by axons that cross the boundaries between them. Previously, we showed that glial segregation at MEP TZs is controlled by a CNS-derived glial population, MEP glia (Smith et al., 2014). In this paper, we extend these studies to show that PNS glia are restricted from migrating into the spinal cord by a distinct glial-glial interaction mediated by radial glial cells. We demonstrate that early in development, PNS cells are able to migrate into and back out of the spinal cord. However, by 48 hpf, when radial glial endfeet occupy the basal edge of the spinal cord, PNS cells can no longer enter the spinal cord, suggesting that interactions between peripheral cells and radial glia are required to maintain the strict cellular boundary between the CNS and PNS. To test this hypothesis, we generated a transgenic zebrafish line that allows for temporal control of radial glial ablation. With this line, we show that in the absence of radial glia, MEP glia enter the spinal cord during a temporal window when they are normally restricted or not competent to enter (Fig. 9). Upon entry, these cells remain within the spinal cord and do not appear to elicit an immune response. These results highlight that the segregation of glial cells at the MEP TZ requires three distinct glial cell populations: MEP glia, which restrict OPCs from exiting the CNS and radial glia, which likely prevent PNS glia from entering the spinal cord (Fig. 9).

Developmental Role of Neural Crest Migration into the Spinal Cord

Surprisingly, during our early imaging of the MEP TZ, we observed neural crest cells migrating into the spinal cord via the MEP TZ (Fig. 2). It is well established that neural crest cells generate multiple peripheral cell types including pigment cells, ensheathing glia and sensory and autonomic neurons (Le Douarin et al., 1991). This lineage of cells is

hypothesized to be fate committed early in migration, but it is possible that subpopulations of these cells could be influenced by factors that are experienced while in the spinal cord, or reciprocally, could influence development of CNS cell populations.

Our time-lapse imaging data showed that after 48 hpf, neural crest cells no longer enter the spinal cord. This time point correlates with the appearance of MEP glia, which replace neural crest cells as the glial cell-type closest to the MEP TZ in the PNS. In our movies, when peripheral cells entered the spinal cord, it was always the cell closest to the MEP TZ that migrated into the CNS. Whether neural crest cells and MEP glia can both enter the spinal cord upon perturbation of radial glia is still unanswered. Unfortunately, our experimental paradigm limited us from addressing this question because we could not induce cell death in radial glia before MEP glia replace neural crest-derived cells at the MEP TZ without also significantly reducing the number of motor neurons in the spinal cord, which would have a profound effect on MEP TZ. However, given the reports that Schwann cells are observed inside the spinal cord in certain disease states (Blakemore and Patterson, 1975; Blakemore, 1976; Duncan et al., 1988; Duncan and Hoffman, 1997), we hypothesize that in addition to MEP glia, neural crest cells can also enter the spinal cord.

Boundary Control and Unidirectional Movement

How do cells come to reside on the correct side of the MEP TZ during development? This study introduces a population of cells that aids in segregating central and peripheral glia (Fig. 9). Previously, examples of ectopic entry of peripheral cells into the spinal cord have been largely correlated with the disruption of astrocytes in mature nervous systems (Blakemore and Patterson, 1975; Blakemore, 1976; Duncan et al., 1988; Duncan and Hoffman, 1997). Our results, collected from an immature nervous system, may highlight the difference in boundary patrol between the developing and mature adult spinal cord. Future studies elucidating the molecular mechanisms that mediate boundary control during development and in a mature nervous system, could reveal interesting, age-dependent aspects of cellular restriction in the spinal cord. Interestingly, a recent study showed, similar to our findings, mutant mice that disrupt radial glia have ectopic PNS cells inside the spinal cord (Zhu et al., 2015). Although there is no direct evidence (i.e. time-lapse imaging) in mice that PNS cells develop normally and then ectopically migrate into the spinal cord after radial glia are disrupted, there is clear evidence to show a cell-autonomous role of radial glia in ensuring PNS cells are restricted to the periphery during development (Zhu et al., 2015). These studies, taken together with the time-lapse imaging results from our studies, demonstrate that radial glia restrict PNS cells from migrating into the spinal cord during development.

Our study also raises another interesting conclusion; migration across the MEP TZ is selective and unidirectional. In this study, we show that the radial glial boundary is established by 48 hpf. Previously, we showed that MEP glia, which function to prevent OPCs from exiting the spinal cord, migrate out of the MEP after 48 hpf, which is also the developmental stage when perineurial glia exit the spinal cord (Kucenas et al., 2008; Smith et al., 2014). Our data demonstrate an intriguing phenomenon where specific cell populations are free to migrate out of the spinal cord, but their re-entry is prohibited. These

results lead us to hypothesize that there is normally not only selective migration across the MEP TZ, but also unidirectional movement. This current study demonstrates that at least one mechanism controlling this unidirectional movement is mediated by radial glia. We note, however, that the lack of OPC migration out of the spinal cord may also be a result of the impact of radial glia on general OPC migration, similar to neuronal migration along radial glia in the cortex (Rakic, 1972).

Beyond CNS/PNS gatekeepers, the role of radial glial cells in spinal cord development has been largely elusive. In our companion paper, we show that radial glial cells represent a common precursor population for CoSa interneurons, secondary motor neurons and oligodendrocytes. Of interest to this study is the reduction of mature oligodendrocytes in the absence of radial glia, which we also see in our MTZ treatment at 24 hpf. Because OPCs and MEP glia display a contact-mediated restrictive behavior (Smith et al., 2014), we hypothesized that OPCs functioned to prevent MEP glia from entering the spinal cord. Our results, however, indicate this hypothesis is unlikely correct since restriction is established before OPCs develop and is still present in the absence of OPCs. With the above data, we conclude that during development, radial glia are likely the cell-type that restricts PNS glia from ectopically entering the spinal cord and play a key role in building a conserved architectural feature of the vertebrate nervous system.

Supplementary Material

Refer to Web version on PubMed Central for supplementary material.

Acknowledgment

The authors would like to thank members of the Kucenas and Barresi laboratories for valuable discussions and Lori Tocke for zebrafish care.

References

Bernardos RL, Raymond PA. GFAP transgenic zebrafish. Gene Expression Patterns. 2006; 6:1007–1013. [PubMed: 16765104]

Binari LA, Lewis GM, Kucenas S. Perineurial glia require Notch signaling during motor nerve development but not regeneration. J Neurosci. 2013; 33:4241–4252. [PubMed: 23467342]

Blakemore WF. Invasion of Schwann cells into the spinal cord of the rat following local injections of lysolecithin. Neuropathol Appl Neurobiol. 1976; 2:21–39.

Blakemore WF, Patterson RC. Observations on the interactions of Schwann cells and astrocytes following X-irradiation of neonatal rat spinal cord. J Neurocytol. 1975; 4:573–585. [PubMed: 1177001]

Coulpier F, Decker L, Funalot B, Vallat JM, Garcia-Bragado F, Charnay P, Topilko P. CNS/PNS boundary transgression by Central Glia in the absence of Schwann cells or Krox20/Egr2 function. J Neurosci. 2010; 30:5958–5967. [PubMed: 20427655]

Coulpier F, Le Crom S, Maro GS, Manent J, Giovannini M, Maciorowski Z, Fischer A, Gessler M, Charnay P, Topilko P. Novel features of boundary cap cells revealed by the analysis of newly identified molecular markers. Glia. 2009; 57:1450–1457. [PubMed: 19243017]

Curado S, Stainier DYR, Anderson RM. Nitroreductase-mediated cell/tissue ablation in zebrafish: A spatially and temporally controlled ablation method with applications in developmental and regeneration studies. Nat Protoc. 2008; 3:948–954. [PubMed: 18536643]

Duncan ID, Hammang JP, Gilmore SA. Schwann cell myelination of the myelin deficient rat spinal cord following X-irradiation. Glia. 1988; 1:233–239. [PubMed: 2976042]

Duncan ID, Hoffman RL. Schwann cell invasion of the central nervous system of the myelin mutants. J Anat. 1997; 190:35–49. [PubMed: 9034880]

Ellett F, Pase L, Hayman JW, Andrianopoulos A, Lieschke GJ. mpeg1 promoter transgenes direct macrophage-lineage expression in zebrafish. Blood. 2011; 117:e49–e56. [PubMed: 21084707]

Emery B. Regulation of oligodendrocyte differentiation and myelination. Science. 2010; 330:779–782. [PubMed: 21051629]

Fraher JP. Axon-glial relationships in early CNS-PNS transitional zone development: An ultrastructural study. J Neurocytol. 1997; 26:41–52. [PubMed: 9154528]

Fraher JP, Kaar GF. The lumbar ventral root-spinal cord transitional zone in the rat. A morphological study during development and at maturity. J Anat. 1986; 145:109–122. [PubMed: 3429297]

Fraher JP, Rossiter JP. Cell clusters on fetal rat ventral roots: Prenatal development. J Anat. 1983; 136:111–128. [PubMed: 6833113]

Honjo Y, Kniss J, Eisen JS. Neuregulin-mediated ErbB3 signaling is required for formation of zebrafish dorsal root ganglion neurons. Development. 2008; 135:2993–2993.

Hughes EG, Kang SH, Fukaya M, Bergles DE. Nat Neurosci. 2013; 16:668–676. 3390(1). [PubMed: 23624515]

Itoyama Y, Webster HD, Richardson EP, Trapp BD. Schwann cell remyelination of demyelinated axons in spinal cord multiple sclerosis lesions. Ann Neurol. 1983; 14:339–346. [PubMed: 6195956]

Jessen KR, Mirsky R. The origin and development of glial cells in peripheral nerves. Nat Rev Neurosci. 2005; 6:671–682. [PubMed: 16136171]

Johnson K, Moriarty C, Tania N, Ortman A, Dipietrantonio K, Edens B, Eisenman J, Ok D, Krikorian S, Barragan J, Gole C, Barresi MJF. Kif11 dependent cell cycle progression in radial glial cells is required for proper neurogenesis in the zebrafish neural tube. Dev Biol. 2013:1–20.

Kim H, Shin J, Kim S, Poling J, Park H-C, Appel B. Satir P, Fallon JF. Notch-regulated oligodendrocyte specification from radial glia in the spinal cord of zebrafish embryos. Dev Dyn. 2008; 237:2081–2089. [PubMed: 18627107]

Kimmel CB, Ballard WW, Kimmel SR, Ullmann B, Schilling TF. Stages of embryonic development of the zebrafish. Dev Dyn. 1995; 203:253–310. [PubMed: 8589427]

Kirby BB, Takada N, Latimer AJ, Shin J, Carney TJ, Kelsh RN, Appel B. In vivo time-lapse imaging shows dynamic oligodendrocyte progenitor behavior during zebrafish development. Nat Neurosci. 2006; 9:1506–1511. [PubMed: 17099706]

Kucenas S, Takada N, Park H-C, Woodruff E, Broadie K, Appel B. CNS-derived glia ensheath peripheral nerves and mediate motor root development. Nat Neurosci. 2008; 11:143–151. [PubMed: 18176560]

Kucenas S, Wang W-D, Knapik EW, Appel B. A selective glial barrier at motor axon exit points prevents oligodendrocyte migration from the spinal cord. J Neurosci. 2009; 29:15187–15194. [PubMed: 19955371]

Le Douarin N, Dulac C, Dupin E, Cameron-Curry P. Glial cell lineages in the neural crest. Glia. 1991; 4:175–184. [PubMed: 1827777]

Maro GS, Vermeren M, Voiculescu O, Melton L, Cohen J, Charnay P, Topilko P. Neural crest boundary cap cells constitute a source of neuronal and glial cells of the PNS. Nat Neurosci. 2004; 7:930–938. [PubMed: 15322547]

McGraw HF, Snelson CD, Prendergast A, Suli A, Raible DW. Postembryonic neuronal addition in Zebrafish dorsal root ganglia is regulated by Notch signaling. Neural Dev. 2012; 7:23. [PubMed: 22738203]

Myers PZ, Eisen JS, Westerfield M. Development and axonal outgrowth of identified motoneurons in the zebrafish. J Neurosci. 1986; 6:2278–2289. [PubMed: 3746410]

Park H-C, Mehta A, Richardson JS, Appel B. olig2 Is required for zebrafish primary motor neuron and oligodendrocyte development. Dev Biol. 2002; 248:356–368. [PubMed: 12167410]

Peri F, Nüsslein-Volhard C. Live imaging of neuronal degradation by microglia reveals a role for v0-ATPase a1 in phagosomal fusion in vivo. Cell. 2008; 133:916–927. [PubMed: 18510934]

Prendergast A, Linbo TH, Swarts T, Ungos JM, McGraw HF, Krispin S, Weinstein BM, Raible DW. The metalloproteinase inhibitor Reck is essential for zebrafish DRG development. Development. 2012; 139:1141–1152. [PubMed: 22296847]

Rakic P. Mode of cell migration to the superficial layers of fetal monkey neocortex. J Comp Neurol. 1972; 145:61–83. [PubMed: 4624784]

Raible DW, Eisen JS. Restriction of neural crest cell fate in the trunk of the embryonic zebrafish. Development. 1994; 120:495–503. [PubMed: 8162850]

Raible DW, Wood A, Hodsdon W, Henion PD, Weston JA, Eisen JS. Segregation and early dispersal of neural crest cells in the embryonic zebra-fish. Dev Dyn. 1992; 195:29–42. [PubMed: 1292751]

Smith CJ, Morris AD, Welsh TG, Kucenas S. Barres BA. Contact-mediated inhibition between oligodendrocyte progenitor cells and motor exit point Glia establishes the spinal cord transition zone. PLoS Biol. 2014; 12:e1001961. [PubMed: 25268888]

Takada N, Appel B. Identification of genes expressed by zebrafish oligodendrocytes using a differential microarray screen. Dev Dyn. 2010; 239:2041–2047. [PubMed: 20549738]

Vermeren M, Maro GS, Bron R, McGonnell IM, Charnay P, Topilko P, Cohen J. Integrity of developing spinal motor columns is regulated by neural crest derivatives at motor exit points. Neuron. 2003; 37:403–415. [PubMed: 12575949]

Zawadzka M, Rivers LE, Fancy SPJ, Zhao C, Tripathi R, Jamen F, Young K, Goncharevich A, Pohl H, Rizzi M, Rowitch DH, Kessaris N, Suter U, Richardson WD, Franklin RJM. CNS-resident glial progenitor/stem cells produce Schwann cells as well as oligodendrocytes during repair of CNS demyelination. Stem Cell. 2010; 6:578–590.

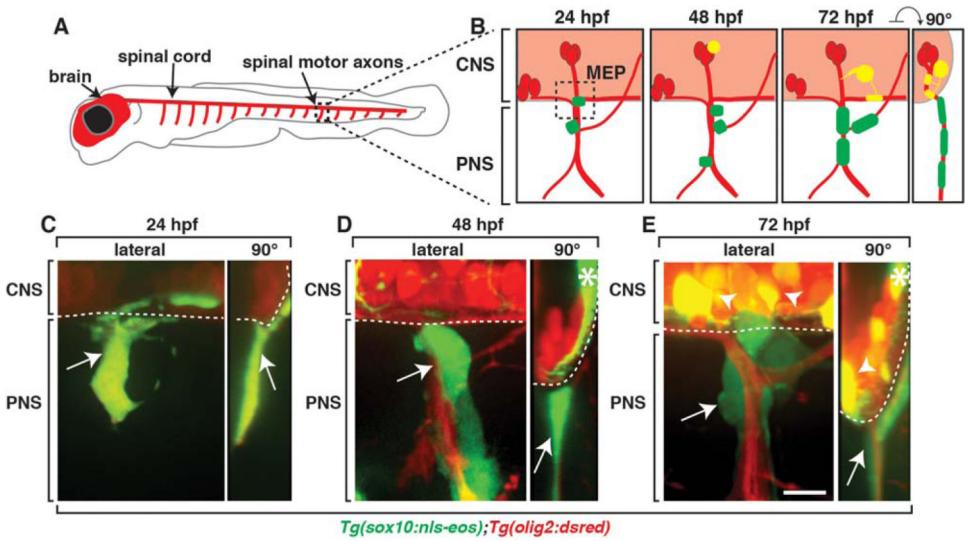

FIGURE 1.

Peripheral and central myelinating glia are segregated at the MEP. A: Schematic of a zebrafish larvae with the brain and spinal cord labeled in red. Boxed region shows the spinal motor nerve roots, which are magnified in B. **B:** Schematics of spinal motor roots at 24, 48, and 72 hpf showing motor axons (red), PNS glia (green) and CNS glia (yellow). Images of *Tg(sox10:eos);Tg(olig2:dsred)* embryos at (**C**) 24, (**D**) 48 (**E**), and 72 hpf. Lateral and cross section (90°) views are shown. Arrows denote peripheral *sox10*$^{+}$ glia and arrowheads denote central *sox10*$^{+}$/*olig2*$^{+}$ OPCs. Asterisks at 48 and 72 hpf denote Eos expression in spinal cord neurons. Dotted lines represents spinal cord boundary. Scale bar, 25 μm.

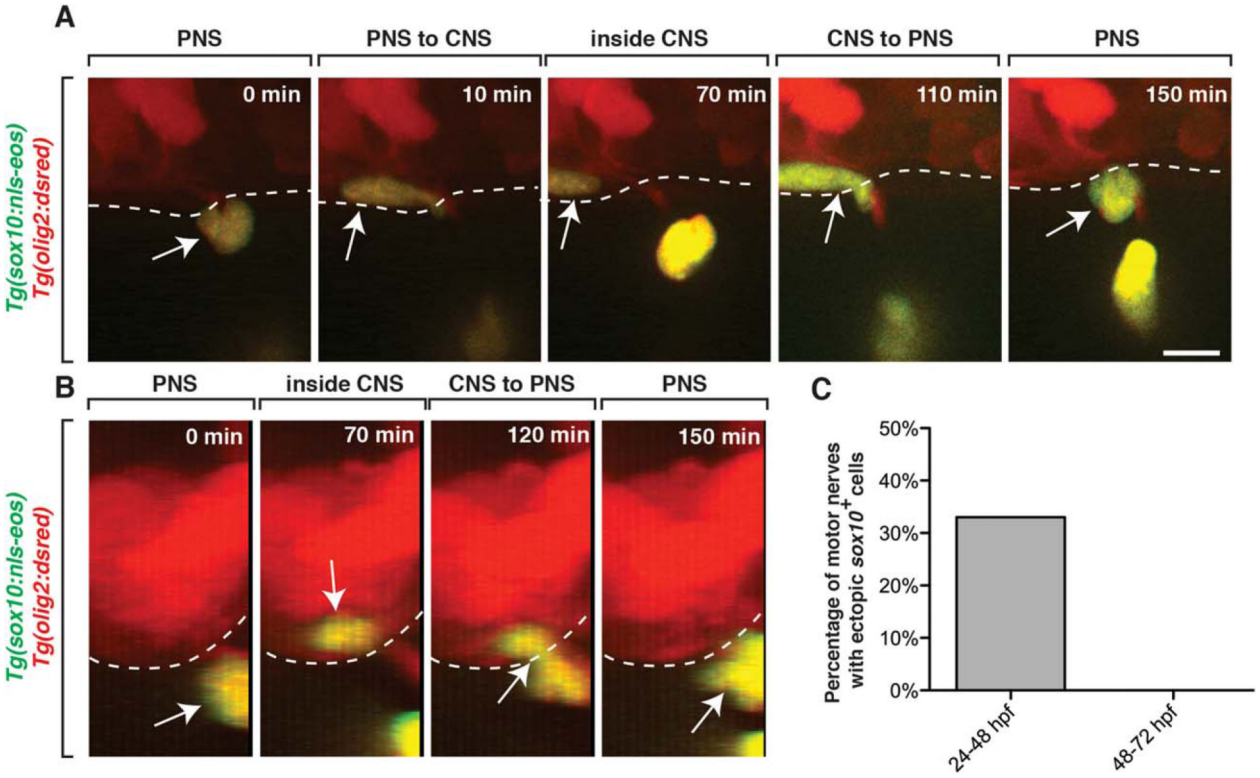

FIGURE 2.

sox10^{+} peripheral cells migrate into the spinal cord during early nervous system development. **A:** Images from a 24 h time-lapse movie starting at 24 hpf of a *Tg(sox10:nls-eos);Tg(olig2:dsred)* embryo. Arrows denote a peripheral *sox10*$^{+}$ cell that entered the spinal cord and then quickly exited. Dashed line denotes edge of spinal cord. **B:** 90-degree digital rotation of images from movie shown in A. **C:** Percentage of the number of nerves that had peripheral *sox10*$^{+}$ cells enter the spinal cord and then exit ($n = 9$). Scale bar, 25 μm.

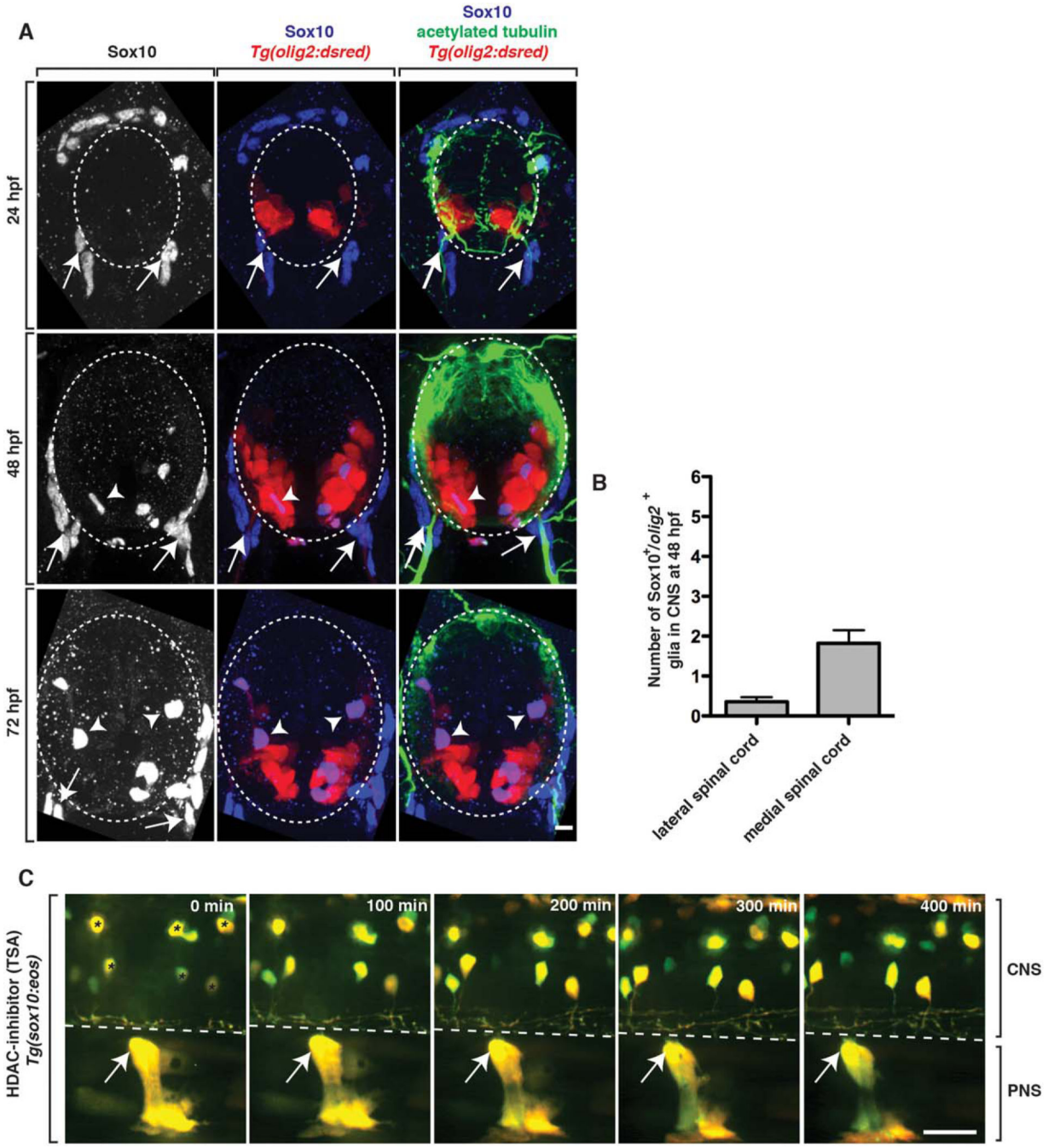

FIGURE 3.

OPCs do not restrict ectopic peripheral glial migration. **A:** Images from 24, 48, and 72 hpf *Tg(olig2:dsred)* embryos stained with antibodies specific to acetylated tubulin (green) and Sox10 (blue). Arrows show peripheral Sox10$^+$ cells while arrowheads denote centrally-located Sox10$^+$ cells. **B:** Quantification of the location of Sox10$^+$ OPCs in the spinal cord at 48 hpf. **C:** Images from a 24 h time-lapse movie starting at 48 hpf of a *Tg(sox10:eos)* embryo treated with TSA at 36 hpf. Arrows denote PNS glia that do not migrate into the

spinal cord. Asterisks indicate *sox10*$^{+}$ neurons that are labeled by *Tg(sox10:eos)*. Dashed lines and circles denote boundary of spinal cord. Scale bars, 25 μm.

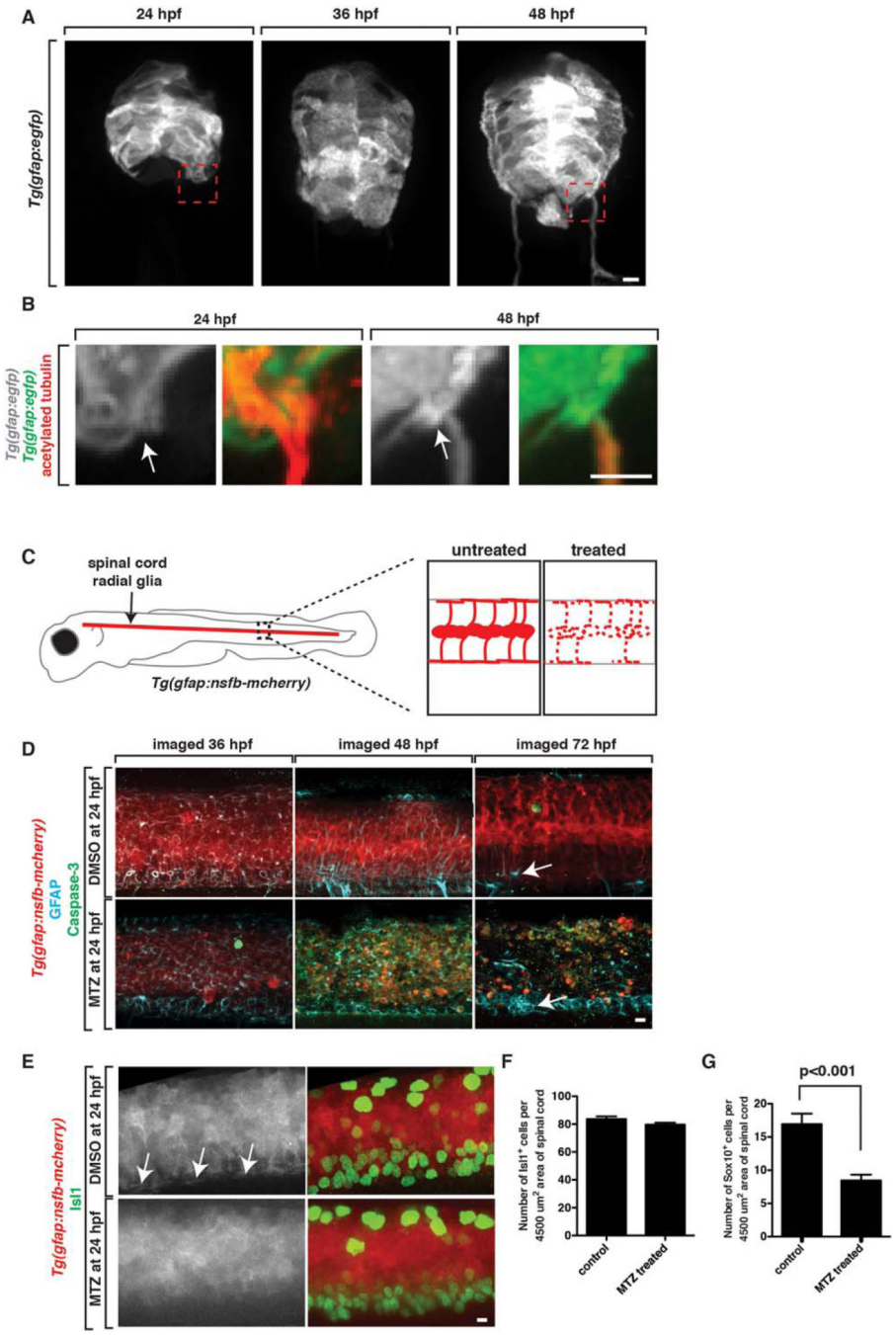

FIGURE 4.

Radial glial cells are specifically ablated in *Tg(gfap:nsfB-mcherry)* embryos. **A:** Images from *Tg(gfap:egfp)* embryos at 24, 36, and 48 hpf. Box denotes location of MEP TZ shown in B. **B:**. Zoomed images of *Tg(gfap:egfp)* embryos stained with an antibody to acetylated tubulin to mark motor axons. Arrow denotes location of MEP. **C:** Schematic of *Tg(gfap:nsfB-mcherry)* embryo with zoomed-in views of the spinal cord in untreated and MTZ-treated animals showing death (dashed lines) of radial glial cells in MTZ-treated animals. **D:** Confocal images of *Tg(gfap:nsfB-mcherry)* animals treated with DMSO or

MTZ at 24 hpf and fixed and stained with antibodies specific to GFAP and Caspase-3 at 36, 48, and 72 hpf. Arrow denotes floorplate radial glia that do not express NTR and are present after MTZ-treatment. **E:** Confocal images of *Tg(gfap:nsfB-mcherry)* animals treated with DMSO or MTZ at 24 hpf and fixed and stained with antibodies specific to Isl1 and Sox10 at 56 hpf. Images show *mcherry*$^{+}$ endfeet (denoted with arrows) in control animals that are absent in MTZ-treated animals. Quantification of (**F**) Isl1^{+} motor neurons (G) and Sox10^{+} glia in the spinal cord at 56 hpf in DMSO and MTZ-treated embryos. Scale bars, 25 μm.

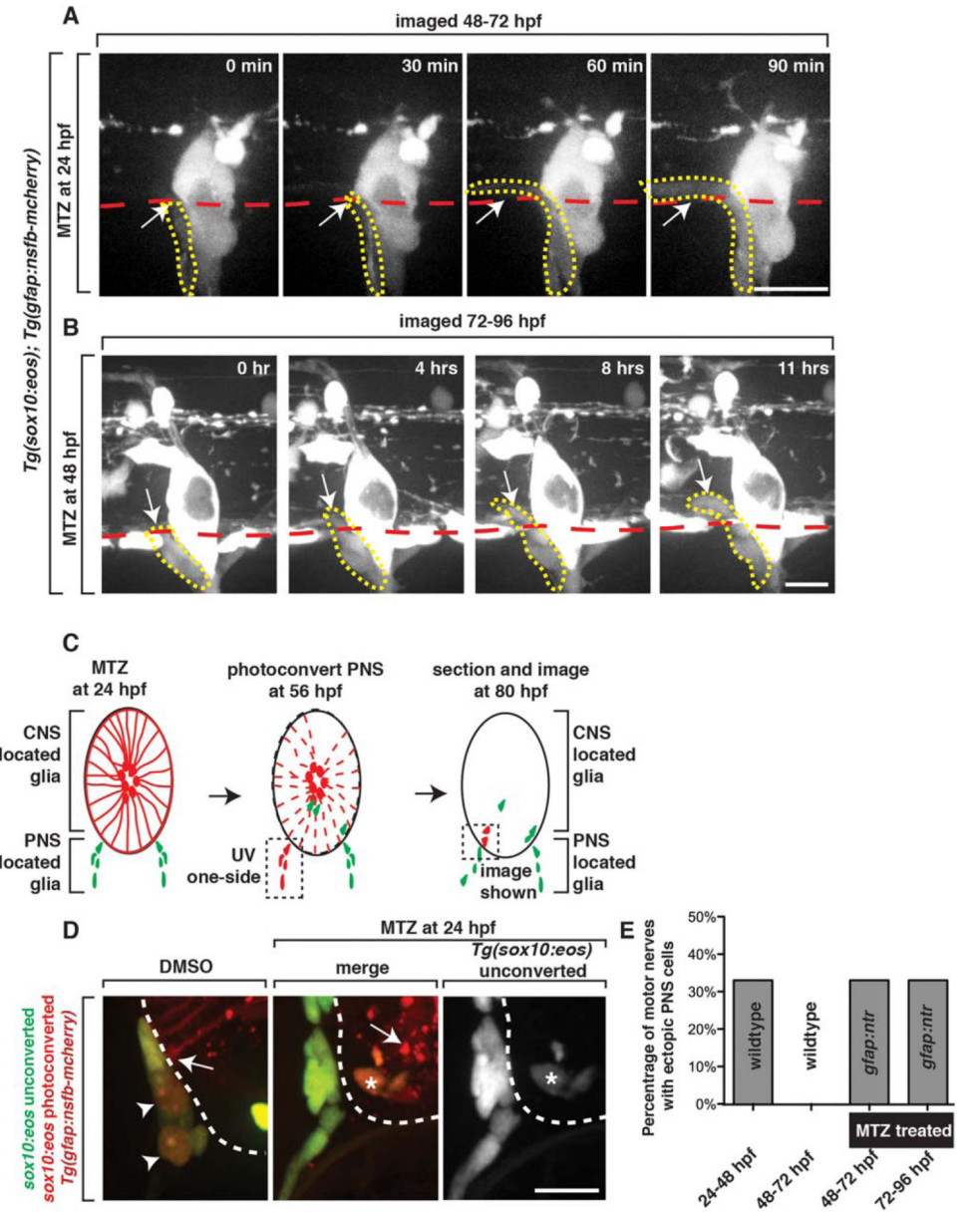

FIGURE 5.

Radial glia are required to restrict ectopic peripheral glial migration into the spinal cord. **A:** Images from a 24-h time-lapse of a *Tg(sox10:eos)* embryo treated at 24 hpf with MTZ and imaged from 48 to 72 hpf. Arrow denotes peripheral *sox10*$^{+}$ cell that migrated into the spinal cord. Red dashed line denotes the edge of the spinal cord. Yellow dashed line denotes ectopically migrating PNS cell. **B:** Images from a 24-h time-lapse of a *Tg(sox10:eos)* embryo treated at 48 hpf with MTZ and imaged from 72 to 96 hpf. Arrow denotes peripheral *sox10*$^{+}$ cell that migrated into the spinal cord. Red dashed line denotes the edge of the spinal cord. Yellow dashed line denotes ectopically migrating PNS cell. **C:** Schematic of the use of Eos photoconversion to demonstrate that peripheral *sox10*$^{+}$ cells enter the spinal cord. PNS located glia at 48 hpf were photoconverted. **D:** In the experiment outlined in C, unconverted (green) and converted (red) Eos is shown in DMSO and MTZ-treated animals. Only in

MTZ-treated animals are converted (red cells with asterisk) ectopically observed within the spinal cord. Arrowheads denote converted cells in controls that did not enter the spinal cord. Arrows denote radial glia endfeet in DMSO-treated animals and radial glia debris in MTZ-treated animals. Note that the ectopic cell in MTZ-treated animals also express unconverted Eos, distinguishing it from *mcherry*$^{+}$ debris. **E:** Quantification of data from A and B showing the number of times a nerve had a cell ectopically migrate into the spinal cord (n = 6). Scale bars, 25 μm.

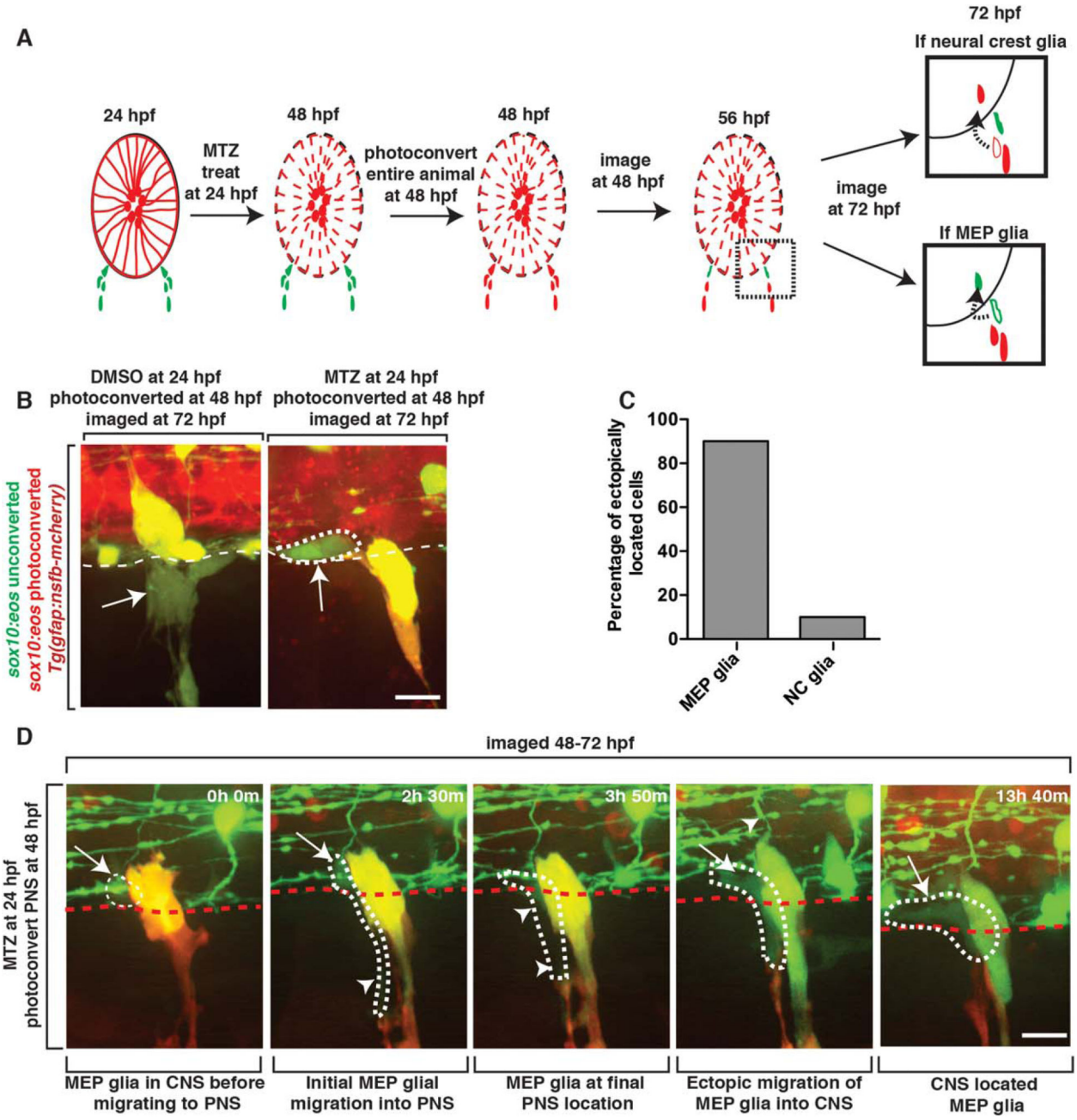

FIGURE 6.

MEP glia migrate into the spinal cord after radial glial ablation. **A:** Schematic of the use of Eos photoconversion to differentially label MEP glia vs neural crest-derived cells. Both potential outcomes are shown at 72 hpf. Arrow denotes migration path of a PNS cell (outlined cell) that has ectopically entered the spinal cord (solid cells). Red cells denote neural crest-derived cells while green cells denote MEP glia. **B:** Images of a *Tg(sox10:eos);Tg(gfap:nsfB-mcherry)* embryo that was treated at 24 hpf with MTZ, photoconverted at 48 hpf and then imaged at 72 hpf. Dotted circle denotes ectopically located *sox10*$^{+}$ cell that is unconverted. **C:** Quantification of experiment described in A and

shown in B. **D:** Images taken from a 24 hour time-lapse of a *Tg(sox10:eos)* embryo, imaged from 48 to 72 hpf, showing an unconverted Eos^{+} cell migrating out of the spinal cord and then back in. Dotted circle marks the cell that ectopically re-enters the spinal cord. Arrow marks the part of the cell that is in the CNS while arrowheads marks the PNS-located side of the cell. Scale bars, 25 μm.

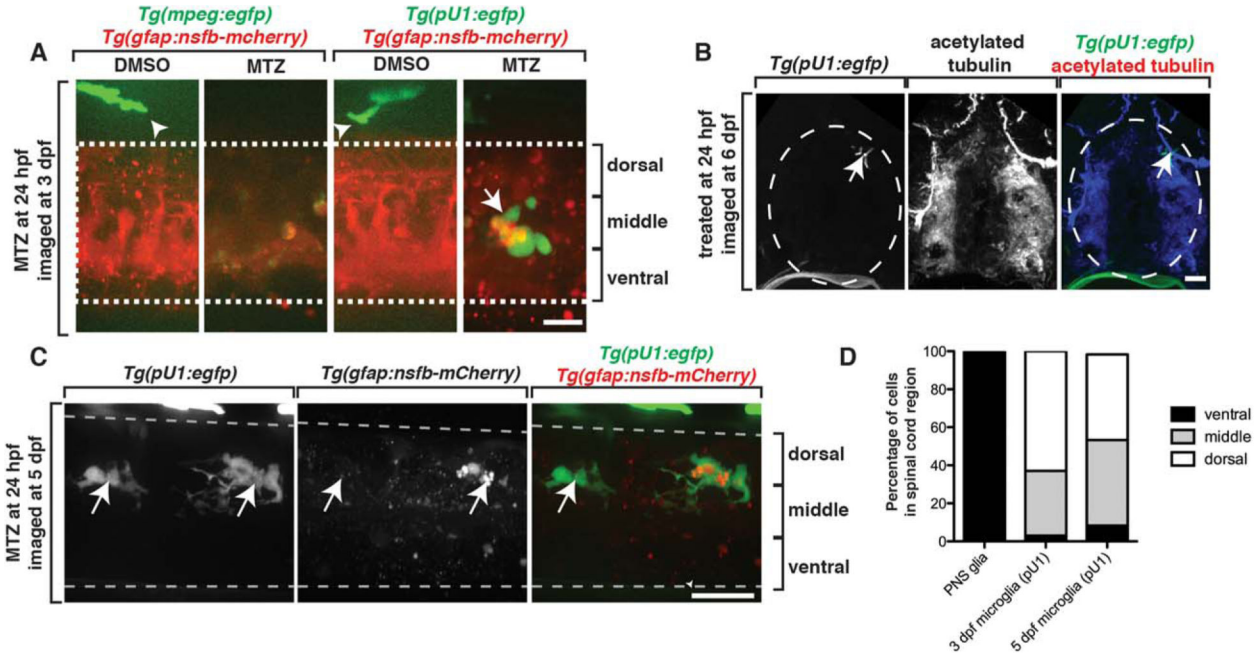

FIGURE 7.

Ectopically located MEP glia do not elicit an immune response. **A:** Images of control and MTZ-treated *Tg(mpeg:egfp);Tg(gfap:nsfB-mcherry)* and *Tg(pU1:egfp);Tg(gfap:nsfB-mcherry)* larvae at 3 dpf. Arrowheads denote macrophages outside of the spinal cord. Arrow denotes microglia inside the spinal cord. Dashed lines denote the edge of the spinal cord. **B:** Transverse sections through *Tg(pU1:egfp)* embryos that were fixed at 5 dpf and stained with an antibody specific to acetylated tubulin. Arrow denotes location of microglia. **C:** Images of a *Tg(pU1:egfp);Tg(gfap:nsfB-mcherry)* embryo treated with MTZ at 24 hpf and imaged at 5 dpf. Arrows denote microglia. Note the lack of $mcherry^{+}$ debris. **D:** Quantification of the location of microglia and ectopically located MEP glia within the spinal cord in MTZ-treated embryos at 3 and 5 dpf. Scale bars, 25 μm.

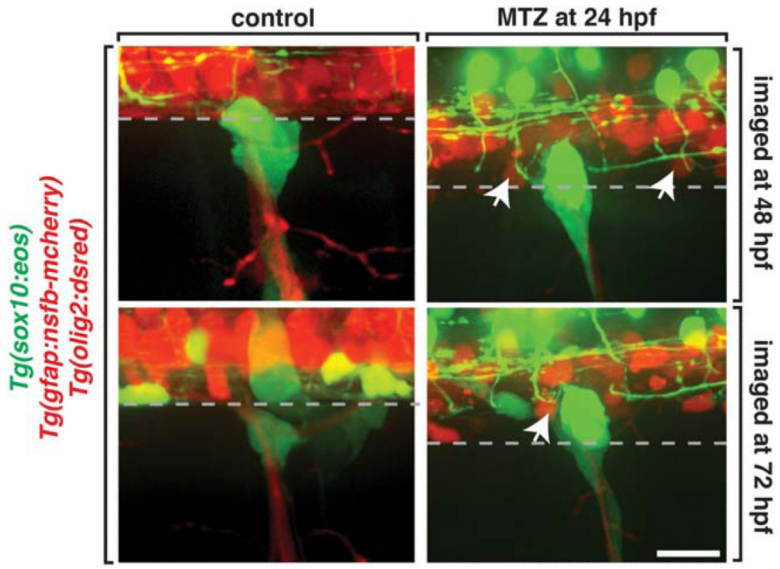

FIGURE 8.

Radial glia selectively gate entrance into the spinal cord. Images of control and MTZ-treated Tg(sox10:eos);Tg(olig2:dsred);Tg(gfap:nsfB-mcherry) embryos. Arrows denote *olig2*$^{+}$ cells within the spinal cord. Dashed line denotes the edge of the spinal cord. Scale bar, 25 μm.

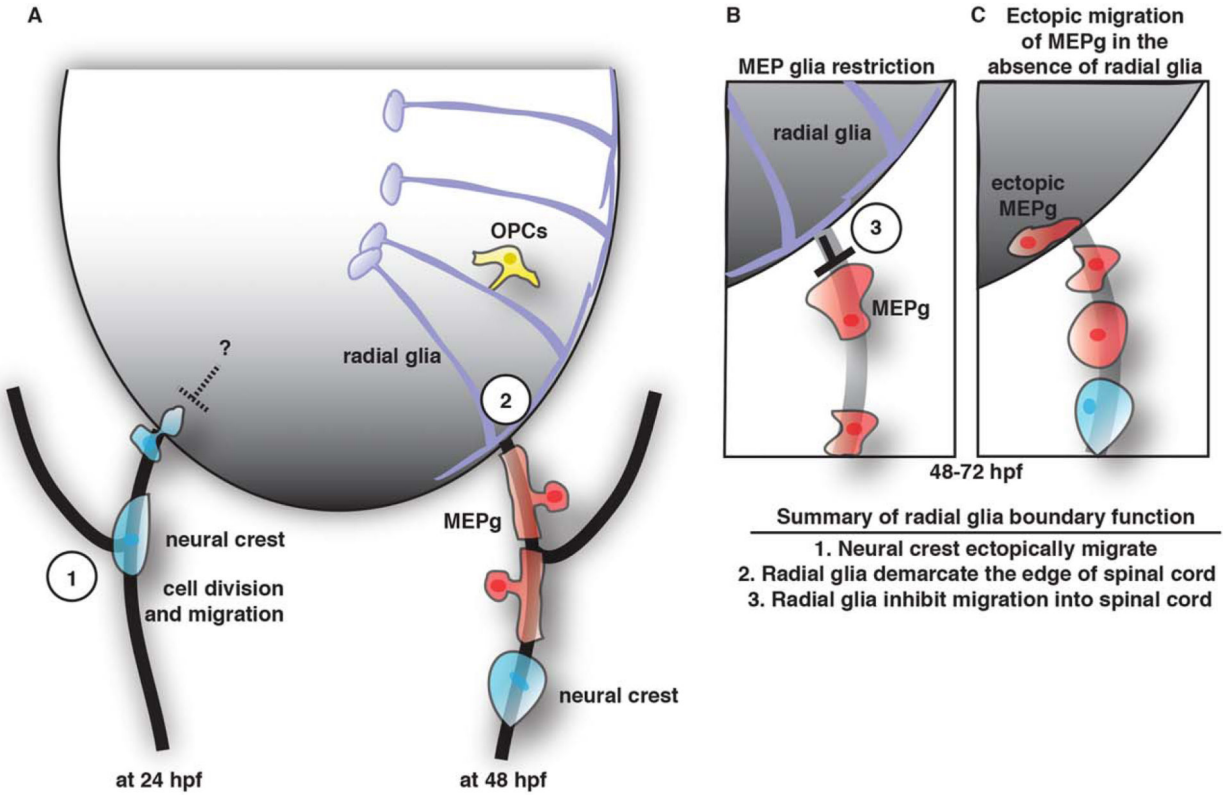

FIGURE 9.

Summary of MEP glia development and function. **A:** Schematic summary the development of the MEP. On the left is a snapshot of a spinal motor nerve at 24 hpf showing neural crest cells can ectopically migrate into the spinal cord but are ultimately restricted by an unknown mechanism. On the right is a snapshot of a spinal motor nerve at 48 hpf showing MEP glia (MEPg, red cells) and neural crest cells (blue) in the PNS and radial glia (purple cells) and OPCs (yellow) in the CNS. **B:** Schematic view of the motor exit point showing MEPg (red cells) are inhibited from entering the spinal cord by radial glia (purple cells). **C:** In the absence of radial glia, MEPg (red cells) enter the spinal cord ectopically.

TABLE 1

Descriptions and abbreviations of transgenic lines used in this study

Transgene Name	Transgene abbreviation	Cell Labeled	Transgene action
Tg(sox10(4.9):nls-eos)	*Tg(sox10:nls-eos)*	Neural crest, Schwann cells and OPCs	Nuclear localized Eos expression in *sox10*$^{+}$ cells
Tg(sox10(4.9):eos)	*Tg(sox10:eos)*	Neural crest, Schwann cells and OPCs	Eos expression in *sox10*$^{+}$ cells
Tg(olig2:dsred2)	*Tg(olig2:dsred)*	Motor neurons/axons and OPCs	DsRed2 expression in *olig2*$^{+}$ cells
Tg(gfap:egfp)	*Tg(gfap:egfp)*	Radial glia	eGFP expression in *gfap*$^{+}$ cells
Tg(gfap:nsfb-mcherry)	*Tg(gfap:nsfb-mcherry)*	Radial glia	NTR expression in *gfap*$^{+}$ cells
Tg(spi1b:gal4 + UAS:egfp)	*Tg(pU1:egfp)*	Microglia and macrophages	eGFP expression in *pU1*$^{+}$ cells
Tg(mpeg-1:egfp)	*Tg(mpeg-1:egfp)*	Macrophages	eGFP expression in *mpeg-1*$^{+}$ cells
Tg(nbt:dsred)	*Tg(nbt:dsred)*	Motor neurons/axons	DsRed expression in *nbt*$^{+}$ cells

All lines used were stable, germline transgenics. Cell types listed for each transgene are only those pertinent to this study.